Scaffold association factor B (SAFB) is required for expression of prenyltransferases and RAS membrane association

Mo Zhou[a], Leena Kuruvilla[b], Xiarong Shi[b], Stephen Viviano[b], Ian M. Ahearn[a], Caroline R. Amendola[a], Wenjuan Su[a], Sana Badri[a], James Mahaffey[a], Nicole Fehrenbacher[a], Jane Skok[a], Joseph Schlessinger[b], Benjamin E. Turk[b], David A. Calderwood[b,c], and Mark R. Philips[a,1]

[a]Perlmutter Cancer Center, NYU Langone Health, New York, NY 10016; [b]Department of Pharmacology, Yale School of Medicine, New Haven, CT 06510; and [c]Department of Cell Biology, Yale School of Medicine, New Haven, CT 06510

Edited by Douglas R. Lowy, National Cancer Institute, Bethesda, MD, and approved October 20, 2020 (received for review March 26, 2020)

Inhibiting membrane association of RAS has long been considered a rational approach to anticancer therapy, which led to the development of farnesyltransferase inhibitors (FTIs). However, FTIs proved ineffective against *KRAS*-driven tumors. To reveal alternative therapeutic strategies, we carried out a genome-wide CRISPR-Cas9 screen designed to identify genes required for KRAS4B membrane association. We identified five enzymes in the prenylation pathway and SAFB, a nuclear protein with both DNA and RNA binding domains. Silencing *SAFB* led to marked mislocalization of all RAS isoforms as well as RAP1A but not RAB7A, a pattern that phenocopied silencing *FNTA*, the prenyltransferase α subunit shared by farnesyltransferase and geranylgeranyltransferase type I. We found that SAFB promoted RAS membrane association by controlling FNTA expression. *SAFB* knockdown decreased GTP loading of RAS, abrogated alternative prenylation, and sensitized *RAS*-mutant cells to growth inhibition by FTI. Our work establishes the prenylation pathway as paramount in KRAS membrane association, reveals a regulator of prenyltransferase expression, and suggests that reduction in FNTA expression may enhance the efficacy of FTIs.

KRAS | RAS | prenyltransferase | farnesyltransferase | SAFB

Mutations of *RAS* genes contribute to human cancer more often than those of any other oncogene, driving a quest for therapeutic strategies that inhibit the function of oncogenic RAS (1). RAS proteins are small GTPases that operate as binary molecular switches to regulate pathways critical for cell proliferation and survival. RAS proteins can signal only when associated with cellular membranes (2, 3). Membrane association of RAS occurs by virtue of a series of critical posttranslational modifications (4). The four RAS proteins, HRAS, NRAS, KRAS4A, and KRAS4B, are ≥92% identical in their G domains but differ substantially in a C-terminal hypervariable region (HVR). Whereas several modifications of the HVR that vary among isoforms direct protein trafficking (5, 6), modification of a CaaX sequence (cysteine, aliphatic × 2, variable) at the C terminus is universal and absolutely required for membrane association (4). A large family of proteins, including RAS proteins and most of the >150 related small GTPases, terminate in a CaaX sequence. Nascent proteins that terminate in CaaX are substrates for a series of three modifications that include addition of a 15- or 20-carbon polyisoprene lipid to the cysteine (prenylation), endoproteolysis of the aaX amino acids, and carboxylmethylation of the newly C-terminal prenylcysteine. These modifications are catalyzed respectively by one of two prenyltransferases (farnesyltransferase [FTase] or geranylgeranyltransferase type 1 [GGTase I]), RAS-converting enzyme 1 (RCE1), and isoprenylcysteine carboxylmethyltransferase (ICMT).

Because RAS proteins require membrane association to function, the prenylation pathway became a target for anti-RAS drugs which led to the development of FTase inhibitors (FTIs) (1, 7). These agents lacked efficacy in *KRAS*-driven tumors because, although under physiologic conditions KRAS is a substrate for FTase and not GGTase I, when FTase is inhibited, KRAS becomes a substrate for GGTase I in a process referred to as alternative prenylation and thereby retains oncogenic function (8, 9). Thus, FTIs failed not because inhibiting KRAS membrane association to block its function is a flawed idea but, rather, because FTIs were unable to block membrane association of KRAS.

Although the posttranslational modifications of RAS HVRs required for membrane targeting are well characterized and catalyzed by enzymes that are considered targets for anticancer drug discovery, the current understanding of the full complexity of RAS trafficking continues to evolve (10–14), and it is likely that additional components yet to be appreciated contribute to the regulation of this pathway. Accordingly, there may be other strategies for therapeutic intervention in RAS-driven cancers beyond inhibition of FTase. As a means to discover alternative targets, we took an unbiased approach to identify genes required to target KRAS to cellular membranes or stabilize its membrane association. We identified a nuclear factor, SAFB, required for the expression of FNTA, the α subunit of both FTase and

Significance

***RAS* oncogenes have long been a target for rational drug design. Whereas the recent advent of KRAS G12C inhibitors has offered hope for direct targeting of the oncoprotein, this mutation occurs in only 11% of *KRAS*-driven tumors, and it remains clear that multiple orthogonal approaches will be required for definitive therapy. Inhibition of KRAS membrane association is an alternative, complementary approach. Here we identify SAFB, a nuclear DNA/RNA binding protein, as a key regulator of prenyltransferase expression. We show that silencing *SAFB* reduces levels of FNTA, a subunit shared by two prenyltransferases, and thereby sensitizes *KRAS* mutant cancer cells to growth inhibition with farnesyltransferase inhibitors (FTIs). Thus, reducing FNTA expression may be a strategy to enhance the effectiveness of FTIs.**

Author contributions: N.F., J. Skok, J. Schlessinger, B.E.T., D.A.C., and M.R.P. designed research; M.Z., L.K., X.S., S.V., I.M.A., C.R.A., W.S., S.B., and J.M. performed research; M.Z., L.K., X.S., I.M.A., C.R.A., W.S., S.B., J. Skok, B.E.T., D.A.C., and M.R.P. analyzed data; and M.Z., I.M.A., C.R.A., W.S., B.E.T., D.A.C., and M.R.P. wrote the paper.

The authors declare no competing interest.

This article is a PNAS Direct Submission.

[1]To whom correspondence may be addressed. Email: philim01@nyulangone.org.

This article contains supporting information online at https://www.pnas.org/lookup/suppl/doi:10.1073/pnas.2005712117/-/DCSupplemental.

First published November 30, 2020.

GGTase I. Silencing *SAFB* abrogated alternative prenylation of KRAS and sensitized *KRAS*-driven tumor cells to FTIs, suggesting that therapeutic strategies aimed at reducing FNTA expression are worth pursuing.

Results

To develop an approach for pooled CRISPR/Cas9 screening, we adapted a system previously established in our laboratory that couples membrane association of KRAS4B to a transcriptional readout (14). We engineered a HEK293 cell line harboring an integrated UAS-driven GFP expression cassette to constitutively express a Gal4/VP16-KRAS4B fusion protein that is normally targeted to the plasma membrane (PM) through the native KRAS4B C-terminal sequence (Fig. 1*A*). Under conditions that reduce KRAS4B membrane association, such as treatment with prenyltransferase inhibitors (*SI Appendix*, Fig. S1), the fusion protein is translocated to the nucleus to induce GFP expression. We reasoned that this assay could report conditions that affect the targeting of nascent KRAS4B to the PM (farnesylation, AAX proteolysis, carboxyl methylation, or chaperone-mediated delivery) as well as those that destabilize membrane association once KRAS4B has been delivered to the PM [e.g., phosphorylation of S181 (15)] (Fig. 1*A*). Thus, in principle, this system is capable of identifying genes required at multiple stages for membrane association of KRAS.

To identify such genes, we transduced our reporter cell line with a genome-wide lentiviral CRISPR library (Brunello) that coexpressed Cas9 with a single-guide RNA (sgRNA). Cells were cultured for 9 d to allow gene editing and adaptation and then sorted into GFP-positive and GFP-negative populations. Enrichment of sgRNAs in the GFP-positive population was determined by amplification of the encoding sequence and next-generation sequencing. Substantial enrichment of sgRNAs targeting specific genes in the GFP positive population is revealed by their displacement from the diagonal in a plot of read counts in GFP-positive vs. GFP-negative cells (Fig. 1*B*). As expected, *KRAS* scored positive in our screen because sgRNAs that target KRAS4B result in C-terminally truncated forms of Gal4/VP16-KRAS4B that do not associate with membranes but retain the nuclear localization sequence of Gal4 and transcriptional activation domains. We repeated the screen two additional times (*SI Appendix*, Fig. S2). Statistical analysis of the screening data using RIGER (16) (Dataset S1) revealed six genes that scored as significantly enriched ($P < 0.05$) in all three screens (Fig. 1*B*). Of these, five were genes in the prenylation pathway, confirming the power of the screen and revealing that prenylation is the most sensitive component of the KRAS4B trafficking pathway. The only exception to known prenylation pathway genes was scaffold association factor B (SAFB). SAFB is a nuclear protein that binds both DNA and RNA (*SI Appendix*, Fig. S3). Originally named scaffold association factor because it was thought to preferentially bind AT-rich regions of DNA associated with insoluble arrays of filaments described as the "nuclear matrix," this assignment is now controversial, and numerous associations with DNA, RNA, and other proteins have been reported (17). Our screening results suggest that SAFB has a previously unanticipated effect on KRAS4B localization.

To confirm our screening result, we silenced SAFB with small interfering RNA (siRNA) in our reporter cells and again observed GFP expression (*SI Appendix*, Fig. S4). To further characterize the role of SAFB, we disrupted the *SAFB* gene in U2OS cells by transient transduction with a sgRNA active in the screen and Cas9 protein and obtained a clone with a single base pair deletion in exon 12 that resulted in premature stop codons in exon 13 (*SI Appendix*, Fig. S5). We validated the requirement of SAFB for KRAS4B membrane association by imaging mCherry-KRAS4B localization in live cells. CRISPR-Cas9 mediated deletion of SAFB resulted in marked mislocalization of mCherry-KRAS4B away from the membrane and into the cytosol and nucleoplasm (Fig. 1*C*). Importantly, GFP-SAFB with silent PAM site mutations to make it insensitive to CRISPR rescued mCherry-KRAS4B membrane association (Fig. 1*C*). This phenotype was recapitulated (Fig. 1*D*) by silencing SAFB with siRNA, by treating cells with a farnesyltransferase inhibitor (FTI), and by silencing *FNTA*, the gene that encodes the α subunit shared by farnesyltransferase (FTase) and geranylgeranyltransferase type 1 (GGTase I). We validated knockdown of *SAFB* and *FNTA* in these cells by immunoblot (Fig. 1*D*). Surprisingly, silencing of *SAFB* reduced the levels of FNTA, suggesting a potential mechanism by which SAFB might act on KRAS4B localization.

To characterize the requirement for *SAFB* on prenyltransferase expression, we examined expression in the SAFB-deficient and parental U2OS cells of both α and β subunits of the prenyltransferase family of heterodimeric enzymes (Fig. 2*A*). Silencing *SAFB* decreased expression of FNTA and its two cognate β subunits, FNTB and PGGT1B, but did not affect expression of RabGGTA or RabGGTB, the α and β subunits of geranylgeranyltransferase type II (Fig. 2*A* and *SI Appendix*, Fig. S6). Expression of FNTB and PGGT1B could be rescued by forced reexpression of SAFB. Interestingly, expression of FNTA from a plasmid not only overcame the effects of SAFB knockdown but also restored levels of FNTB and PGGT1B, suggesting that the effect of SAFB on the β subunits is indirect through FNTA. Indeed, silencing FNTA with siRNA diminished expression of FNTB and PGGT1B but not RabGGTA or RabGGTB (*SI Appendix*, Fig. S6). These data are consistent with FNTA acting to stabilize the β subunits by engaging them as heterodimers. Interestingly, silencing FNTB with siRNA enhanced expression of PGGT1B, suggesting that when FNTB is not available to complex with FNTA, more PGGT1B can do so and thereby avoid degradation (*SI Appendix*, Fig. S6). Importantly, the mislocalization of mCherry-KRAS4B into the cytosol upon silencing *SAFB* (Fig. 1*D*) demonstrates that SAFB deficiency abrogates alternative prenylation, a result consistent with the requirement for *FNTA* for both FTase and GGTase I.

To confirm the loss of FTase and GGTase I activity, we determined, by live-cell confocal imaging, the subcellular localization of GFP-tagged small GTPases in parental and SAFB-deficient U2OS cells with and without forced expression of FNTA (Fig. 2*B*). NRAS, HRAS, KRAS4A, and KRAS4B are substrates for FTase (FNTA/FNTB heterodimer). All four RAS proteins were expressed on the PM and endomembranes of parental cells and mislocalized to the cytosol and nucleoplasm in SAFB-deficient cells, in a pattern indistinguishable from that of parental cells treated with FTI. Forced expression of FNTA in SAFB-deficient cells restored membrane association. GFP-RAP1A, a substrate for GGTase I (FNTA/PGGT1B heterodimer), behaved in the same way. In contrast, the subcellular localization on vesicular membranes of GFP-RAB7A, a substrate for GGTase II (RabGGTA/RabGGTB heterodimer), was not affected by silencing *SAFB*. GFP extended with the C-terminal 60aa of RIT, a small GTPase that is not prenylated but instead driven to the PM by an amphipathic C-terminal α helix (18), decorated the PM of the U2OS cells, and this localization was unaffected by silencing *SAFB*. Thus, *SAFB* was required for membrane localization of small GTPase substrates of FTase and GGTase I but not GGTase II, consistent with an effect mediated by regulation of *FNTA* expression.

To validate mislocalization of mCherry-KRAS4B upon SAFB silencing, we examined membrane association of endogenous RAS protein by subcellular fractionation. Parental and SAFB-deficient U2OS cells were disrupted by nitrogen cavitation (19), and membrane pellets were separated from supernatants containing cytosol by centrifugation at 350,000 × *g*. Whereas in parental cells 84% of total RAS was recovered in the membrane

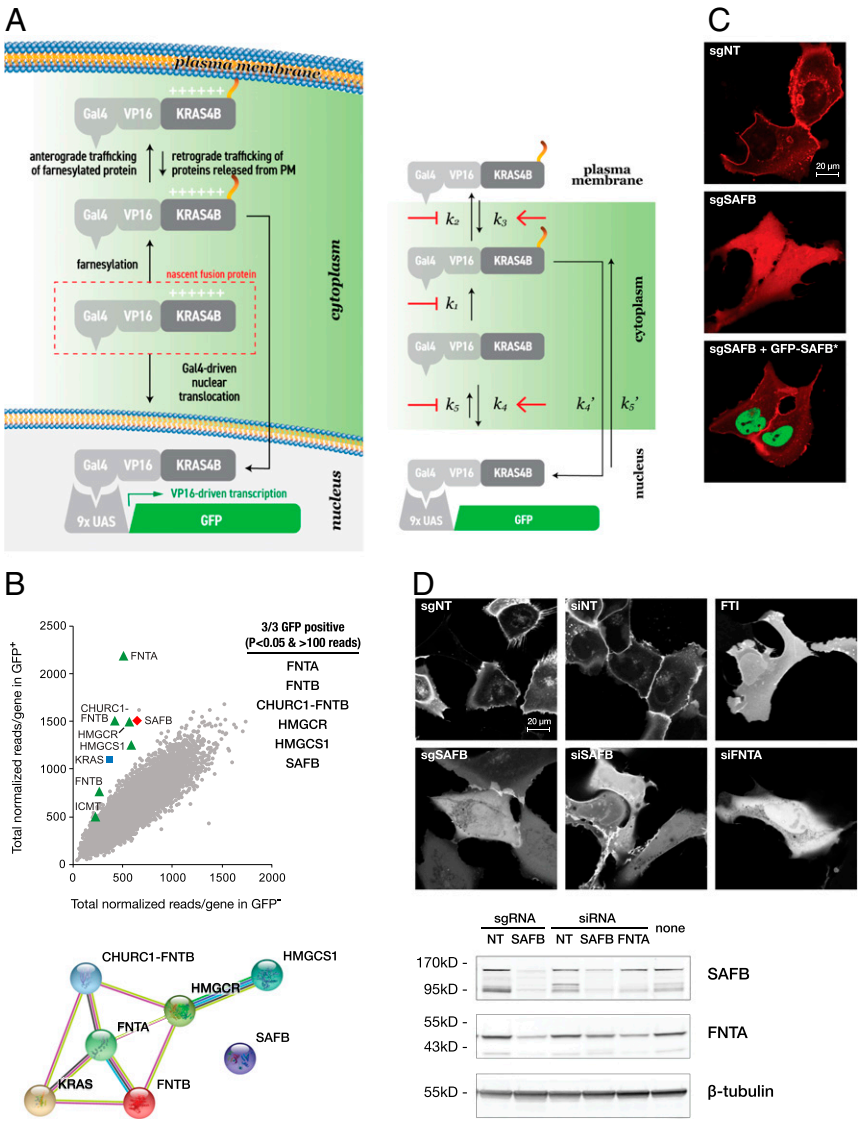

Fig. 1. A genome wide CRISPR screen identifies SAFB as a gene required for KRAS4B membrane association. (*A*) Schematic of the KRAS4B membrane association assay used in the screen (*Left*). At baseline the Gal4-VP16 transcriptional activator module fused to KRAS4B is sequestered from the nucleus by the native membrane-targeting sequence of KRAS4B but induces expression of GFP upon loss of affinity for membranes. The *Right* panel shows the various nodes in the trafficking pathway that, upon inhibition (⊣) or enhancement (←), could lead to increased nuclear import of Gal4-VP16-KRAS4B. (*B*) Results of one of three independent CRISPR screens plotted as read counts for guides targeting each gene in GFP^+ vs. GFP^- cells such that deviation from the diagonal shows enrichment or depletion (*Top*). Listed on the right are the genes that differed significantly with >100 reads in three of three screens, and on the *Bottom* is a STRING protein interaction plot showing that all but SAFB are known components of the polyisoprene biosynthetic pathway. (*C*) U2OS cells edited by CRISPR-Cas9 with either a control (sgNT) or SAFB-targeting guide (sgSAFB) were transfected with either mCherry-KRAS4B alone or mCherry-KRAS4B and GFP-SAFB with a sgSAFB-resistant PAM site and imaged alive with a confocal microscope. (*D*) U2OS cells in which SAFB or the α subunit of FNTA was silenced with CRISPR-Cas9 or siRNA, as indicated, or treated with a FTI, were transfected with mCherry-KRAS4B and imaged alive as in *C* (*Top*). Silencing of SAFB and FNTA was confirmed by immunoblot, shown on the *Bottom*. In *C* and *D* cells representative of >100 per plate are shown. (Scale bar, 20 μm.)

fraction, this was reduced to 59% in SAFB-deficient cells (Fig. 2*C*). Importantly, forced expression of FNTA in SAFB-deficient cells restored the membrane fraction of RAS. Whereas KRAS4B is a substrate for FTase, RAP1 is prenylated by GGTase I. Like KRAS4B, the fraction of RAP1A recovered in the membrane fraction was diminished in SAFB-deficient cells and restored by forced expression of FNTA. These data were supported by an immunoblot with an antibody that recognizes only unprenylated RAP1A (20). Unprenylated RAP1 was detected in the cytosolic fraction of SAFB-deficient but not parental cells and was lost upon forced expression of FNTA. Thus, silencing *SAFB* mislocalized both endogenous KRAS4B and RAP1A as a consequence of loss of prenylation, and basal membrane association of each GTPase could be restored by expression of FNTA, the α subunit required for both forms of prenylation, establishing an epistatic relationship between *SAFB* and *FNTA* in small GTPase membrane association.

To determine whether SAFB controls FNTA expression at the level of transcription, we quantified abundance of prenyltransferase messenger RNA (mRNA) by qRT-PCR in U2OS cells with and without silencing of *SAFB* with short hairpin RNA (shRNA) (Fig. 3*A*). Three different shRNAs that target *SAFB* reduced *FNTA* mRNA levels almost as much as an shRNA that directly targets *FNTA*. Interestingly, silencing *FNTA* modestly reduced *FNTB* mRNA abundance, suggesting a feed-forward mechanism whereby prenylation of some substrate(s) is required

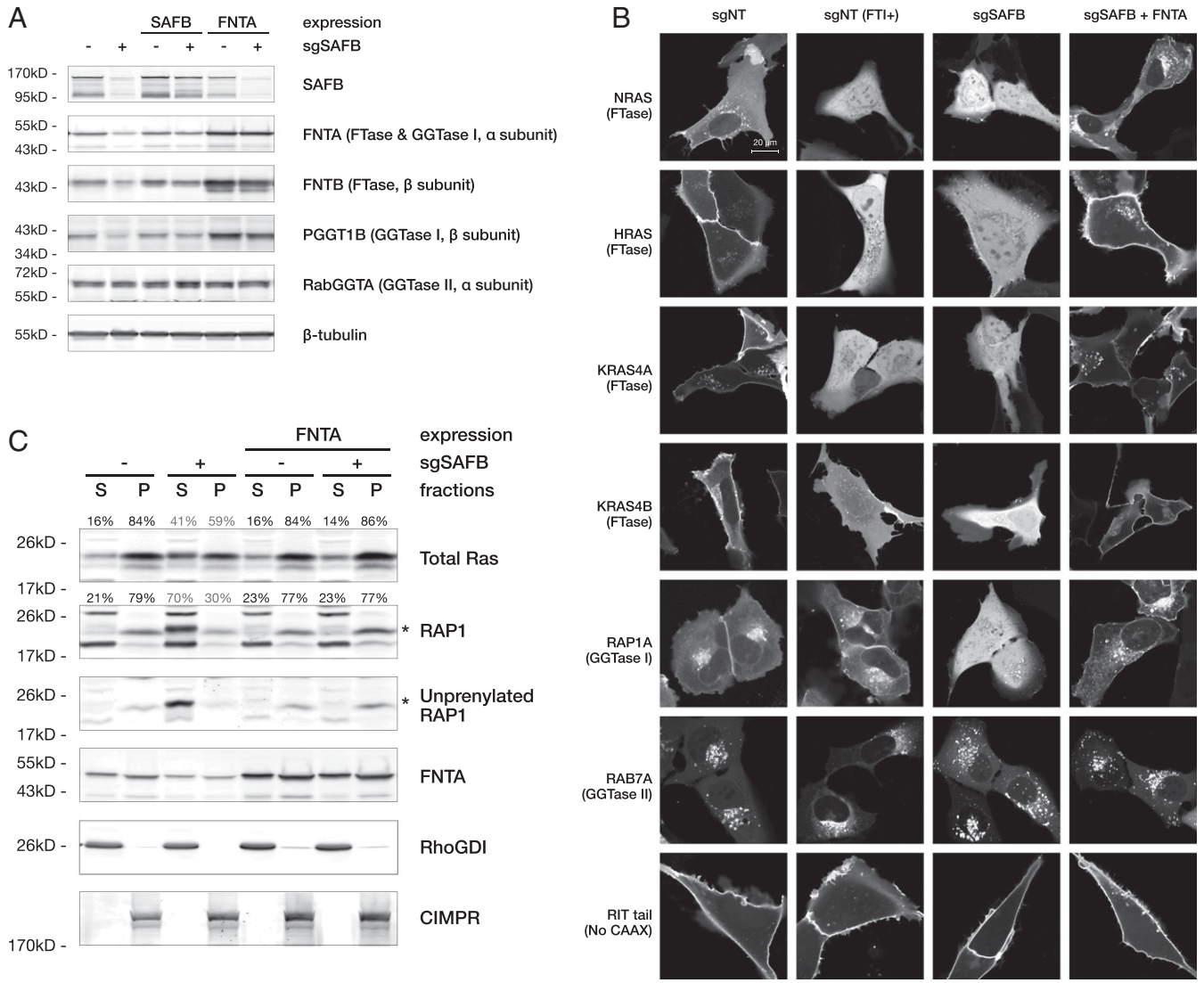

Fig. 2. Loss of SAFB reduces levels of FNTA and mislocalizes prenylated RAS and RHO family GTPases. The genomes of U2OS cells were edited by CRISPR-Cas9 and either nontargeting guides (–) or guides targeting *SAFB* (+) and stably transfected with an empty vector or plasmids directing expression of SAFB or FNTA. (*A*) Cell lysates were analyzed for the indicated prenyltransferase subunits by immunoblots. Data shown are representative of six independent experiments. (*B*) Cells were transiently transfected with the indicated GFP- or mCherry-tagged small GTPases and imaged alive by confocal microscope with or without FTI treatment (25 μM L-744,832). (Scale bar, 20 μm.) (*C*) Membrane association of endogenous RAS and RAP1 determined by subcellular fractionation with or without silencing SAFB as in *A* with or without overexpression of FNTA as indicated. Cells were disrupted by nitrogen cavitation, the postnuclear supernatant was separated into cytosol (S = supernatant) and total membranes (P = pellet) and the indicated proteins assayed by immunoblot. The percentage of RAS and RAP recovered in S vs. P for each condition is shown above each lane as determined by Li-Cor Odyssey scan. Data shown are representative of two independent experiments.

for efficient transcription of *FNTB*. Silencing *SAFB* had a similar effect on *FNTB* mRNA abundance as did silencing *FNTA*, consistent with an indirect effect via *FNTA* knockdown. Silencing neither *FNTA* nor *SAFB* had an effect on the mRNA abundance of any of the other prenyltransferase subunits, PGGT1B, RABGGTA, RABGGTB, and PTAR1 (21). The abundance of HMG-CoA reductase (*HMGCR*) mRNA was minimally affected by loss of *FNTA* or *SAFB*, suggesting feedback regulation by protein prenylation mediated by FNTA. *FNTA* or *SAFB* was dispensable for mRNA expression of RCE1 and ICMT, enzymes required for CaaX processing. These data suggest that *SAFB* is required for *FNTA* transcription and, indirectly, *FNTB* but no other prenyltransferase or CaaX processing gene.

Given the plethora of functions ascribed to SAFB (17), we sought to elucidate the mechanism whereby it regulates expression of FNTA. To determine whether SAFB physically associates with regulatory regions of the *FNTA* gene we analyzed chromosome immunoprecipitation DNA sequencing (ChIP-seq) data available in the Encyclopedia of DNA Elements (ENCODE) Consortium database (Fig. 3 and *SI Appendix*, Fig. S7). SAFB peaks were observed in 3,776 genes (Dataset S2), including *FNTA* on chromosome 8p11.21. The SAFB binding site spans the first exon/intron junction, a region that is coincident with H3K4me1 and H3K27ac peaks often present in enhancers. These data are consistent with SAFB binding to putative regulatory elements in the *FNTA* gene. Other RAS and CaaX processing genes with SAFB binding sites in putative regulatory regions included *HRAS, KRAS, RRAS, RCE1,* and *RABGGTA*. No binding sites were detected in the *FNTB* locus. The ENCODE database also includes RNA-seq in K562 chronic myelogenous

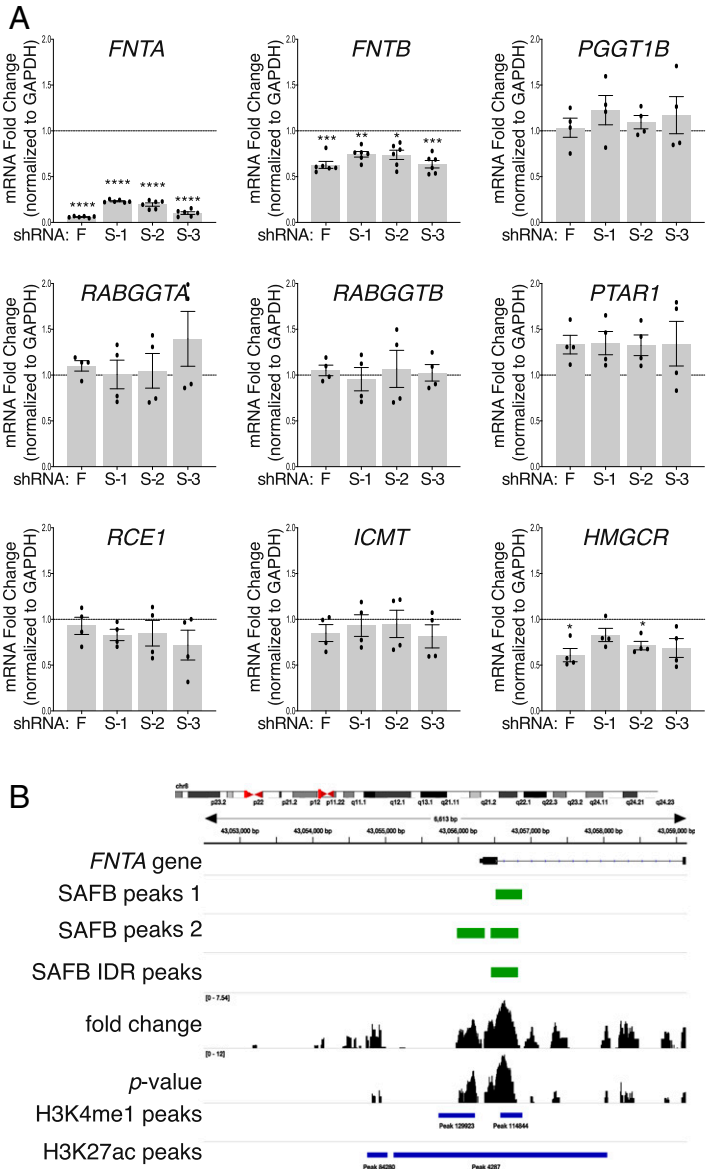

Fig. 3. SAFB regulates *FNTA* mRNA abundance and binds to the *FNTA* locus. (*A*) Stable knockdown of *FNTA* (F) or *SAFB* (S 1-3) was accomplished by lentiviral transduction with the shRNAs indicated or a nontargeting hairpin. mRNA abundance of the indicated genes was measured by qRT-PCR as described in *Methods* and plotted as the fold change relative to noncoding shRNA; $n \geq 4$, $^{****}P < 0.0001$, $^{***}P < 0.001$, $^{**}P < 0.01$, $^{*}P < 0.05$ by paired Student's *t* test. (*B*) SAFB binding to the *FNTA* locus as revealed by ChIP-seq ENCODE data in K562 cells ±disruption of SAFB by CRISPR-Cas9. Pooled fold change in reads over control as well as IDR peaks are plotted along with H3K4me1 and H3K27ac peaks associated with promotor regions on a map of the relevant fragment of chromosome 8.

leukemia cells with and without silencing *SAFB* with CRISPR-Cas9. Analyzing these data and setting a threshold of a q value of <0.05 and $\log_2$ fold change >1, expression of 161 genes was found to be down-regulated, and that of 31 genes was up-regulated upon loss of *SAFB* (Dataset S3). Although neither *FNTA* nor *FNTB* were among these, *HMGCS1* and *HMGCR* were, and importantly, the cholesterol/mevalonate/polyisoprene biosynthesis pathways scored higher than any other in gene ontology analysis (*SI Appendix*, Fig. S9*A*). Interestingly, there was only partial overlap between the genes that bound SAFB and those for which differential expression was observed (*SI Appendix*, Fig. S9*B*). Indeed, the expression of 3,023 genes with SAFB binding sites was unaffected by SAFB deficiency, and conversely, 2,058 genes that were differentially expressed with and without SAFB lacked binding regions for the protein. This is consistent with an earlier study that found no overlap among the 541 promoters that bound SAFB (ChIP-on-chip) and 680 genes differentially regulated upon silencing SAFB (Affimetrix array) (22). Aside from this study and the ENCODE RNA-seq data, one additional study reported differential gene expression before and after silencing SAFB (Gene Expression Omnibus, accession no. GSE125037), this one in AML12 murine hepatocytes in which *SAFB* was knocked down with shRNA (23). Among these three studies, *FNTA* expression was repressed upon loss of SAFB only in the AML12 cells and only by 43% (Dataset S3). Moreover, there is very little overlap among these three sets of SAFB-regulated genes (*SI Appendix*, Fig. S9*C*). Thus, despite our unambiguous observation that *FNTA* expression at the level of both mRNA and protein depends on SAFB, this relationship was not revealed by genome-wide transcriptomic analysis.

Prenylation is required for RAS signaling (2, 3, 24). To determine if SAFB is required for RAS function, we studied GTP-loading and MAPK signaling in parental and SAFB-deficient U2OS cells (Fig. 4). Whereas silencing SAFB had little effect on the relatively low levels of GTP-bound RAS in resting, serum-starved cells, SAFB deficiency reduced epidermal growth factor (EGF)-stimulated loading of RAS with GTP by about 50%. Interestingly, despite diminished GTP loading of RAS, phosphorylation of ERK was only slightly affected. Dissociation of GTP-loading of RAS and ERK phosphorylation has been reported several times in RAS mutant tumor cells (13, 14, 25) and likely reflects either RAS-independent ERK phosphorylation or the fact that residual GTP-loaded RAS is sufficient to sustain signaling.

The effects of SAFB deficiency on membrane localization and GTP loading of RAS suggested that *SAFB* silencing might sensitize cells to FTIs. To test this hypothesis, we studied lung adenocarcinoma cells with and without a *KRAS* mutation. Whereas FTI increased from 20 to 30% the fraction of total RAS recovered in the cytosol of A549 cells, the cytosolic pool increased to 45% in cells in which *SAFB* was silenced with shRNA (Fig. 5*A*). Whereas FTI had no effect on GTP loading of RAS in A549 cells expressing a control shRNA, the drug decreased by 50% the GTP loading of RAS in cells expressing an shRNA targeting *SAFB* (Fig. 5*B*). The 50% inhibitory concentration (IC_{50}) of FTI for inhibition of cell growth in *KRAS* mutant cells was decreased by 12- and 6-fold in A459 and H358 cells, respectively (from 19.6 to 1.7 and 38.8 to 6.3 μM), when *SAFB* was silenced with shRNA (Fig. 5*C*). In contrast, silencing SAFB had no effect on the IC_{50} for growth inhibition by FTI in the KRAS wild-type cell lines H1437 and H1975. Silencing of *SAFB* in these cell lines with consequent decrease in FNTA expression was validated by immunoblot (*SI Appendix*, Fig. S8). To determine whether SAFB deficiency would also sensitize to FTI tumor cells driven by mutant *NRAS*, we studied SKMEL-147 melanoma cells. Indeed, silencing SAFB by siRNA in these cells reduced by sixfold the IC_{50} for FTI (from 0.750 to 0.120 μM) for growth inhibition (*SI Appendix*, Fig. S10). Thus, SAFB deficiency sensitized both *KRAS* and *NRAS* mutant cells to FTI.

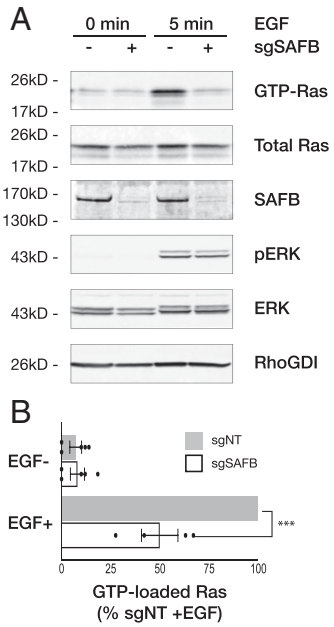

Fig. 4. Loss of SAFB reduces levels of GTP-loaded RAS. U2OS cells edited by CRISPR-Cas9 with nontargeting sgRNAs (–) or those targeting *SAFB* (+) were serum starved and then treated with or without 10 ng/mL EGF for 5 min. (*A*) Lysates were analyzed by immunoblots for the indicated proteins that include GTP-loaded RAS (GTP-RAS) affinity captured by GST-RBD. (*B*) The bar graph of GTP-loaded RAS normalized to total RAS (quantified by Li-Cor Odyssey) represents data from four independent experiments; ***P < 0.001 by paired Student's t test.

Discussion

Applying a relatively stringent threshold in our screen ($P < 0.05$ in each of three replicate screens), we found six genes that, when silenced, diminished KRAS4B association with membranes. Five of these were in the prenylation pathway, including *FNTA* and *FNTB*, which encode the α and β subunits of FTase; *CHURC1-FNTB*, which is a transcript produced as a read through of Churchill domain containing 1 protein and *FNTB* on chromosome 14; HMG-CoA synthase (*HMGCS1*); and HMG-CoA reductase (*HMGCR*). Each of these genes encode enzymes required either for the biosynthesis of polyisoprene lipids (mevalonate pathway) or their covalent conjugation with the cysteine of CaaX sequences. HMGCR catalyzes the rate-limiting step in polyisoprene and cholesterol synthesis and is the target of the statin class of cholesterol-lowering medications. Therefore, its inclusion along with *FNTA* and *FNTB* is not surprising. Although at pharmacologically tolerated doses, statins neither mislocalize small GTPases or affect protein prenylation in vivo, statins applied at higher doses to cultured cells do affect membrane association of RAS proteins (13). It is interesting that HMGCS1, the enzyme immediately upstream of HMGCR in the pathway, met our stringent threshold for SAFB dependence but mevalonate kinase and farnesyl-PP synthase, downstream of HMGCR, did not (although mevalonate kinase scored positive in one of three screens). This may reflect the half-life or the differential kinetics of these enzymes or simply the efficiency or abundance of the sgRNAs in the library. Nevertheless, the identification of multiple nodes in the protein prenylation pathway is both expected and compelling and argues that the screen was robust and that the prenylation pathway is the most sensitive to perturbation in the context of KRAS4B membrane association. It is also noteworthy that no genes were identified that stabilize the association of KRAS4B with membranes following initial targeting (see Fig. 1 for possible modes of increasing nuclear GAL4/VP16-KRAS4B). Because the asymmetric distribution of phosphatidylserine (PS) in the PM has been shown to produce the negative charge that stabilizes KRAS4B association (26), we expected to find genes involved in PS metabolism or transport (27). The only gene in these pathways that scored consistently positive, albeit without passing our stringent RIGER analysis, was PI4KIIIα, which is responsible for generating the pool of PI4P at the PM that is exchanged with PS generated in the ER (28). Because we have shown that phosphorylation of KRAS4B on serine 181 regulates a farnesyl-electrostatic switch (15), we also predicted that a KRAS4B kinase would read out in our screen. However, not only are the classical PKCs that modify KRAS4B redundant, but other kinases such as PKG have been reported to phosphorylate serine 181 of KRAS4B (29).

SAFB was the outlier gene identified in the screen because there is no evidence that this protein is associated with cellular trafficking. Moreover, it was not immediately clear how a nuclear factor could control the membrane association of a small GTPase. The mystery was solved when we discovered that expression of *FNTA* requires *SAFB*. Thus, all of the genes identified at a high level of stringency were in the prenylation pathway, further validating the conclusion that this pathway affords the greatest vulnerability with regard to blocking KRAS association with membranes.

SAFB is a member of a family of three highly homologous paralogs that also include *SAFB2* and SAFB-like transcriptional modulator (*SLTM*) (17). These proteins possess both DNA and RNA binding domains and were initially identified through

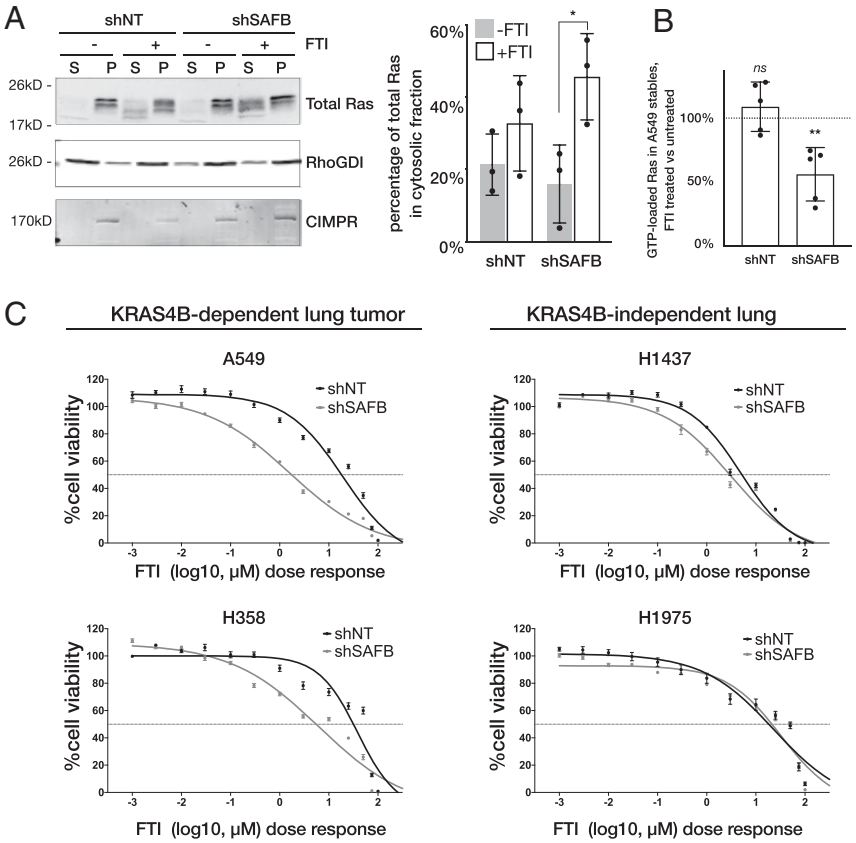

Fig. 5. Loss of SAFB diminishes membrane association and GTP loading of KRAS4B and sensitizes KRAS4B-dependent lung tumor cells to FTI treatment. KRAS4B-dependent (A549, H358) and KRAS4B-independent (H1437, H1975) lung tumor cells were stably transfected with a nontargeting shRNA or one targeting *SAFB* and plated untreated or treated with FTI (L-744,832). (*A*) A549 were disrupted by nitrogen cavitation, separated into S and P fractions by ultracentrifugation, and analyzed by immunoblots for the indicated proteins, including cytosolic (RhoGDI) and membrane (cation-independent manose-6-phosphate receptor; CIMPR) markers (*Left*). Bands were quantified by Li-Cor Odyssey, and percent of total RAS in the cytosol is plotted to the *Right*; $n = 3$, $^{*}P < 0.05$. (*B*) GTP loading of RAS in FTI-treated (25 μM L-744,832) A549 cells normalized to that measured in untreated cells with and without silencing *SAFB* by shRNA. $^{**}P < 0.01$, $n = 5$. (*C*) The viability (normalized to untreated cells) of cells with and without stably silencing *SAFB* by shRNA was determined by 3-(4,5-dimethylthiazol-2-yl)-5-(3-carboxymethoxyphenyl)-2-(4-sulfophenyl)-2H-tetrazolium (MTS) assay after 6 d of treatment with indicated concentrations of FTI (L-744,832), $n = 3$. ns, not significant.

association with AT-rich DNA sequences thought to represent DNA elements of the "nuclear matrix" or "nuclear scaffold" (30). This initially suspected function of SAFB has been refined and substantiated by a recent study demonstrating that SAFB stabilizes heterochromatin architecture (31). However, an exclusive role for SAFB as a nuclear scaffold protein has been called into question by reports that it has a number of additional functions (17). These include regulation of transcription, roles in mRNA processing, and functions mediated by protein–protein interactions (17). Recently, SAFB was found to be among numerous RNA binding proteins packaged into extracellular vesicles in an LC3-dependent manner (32). *SAFB* has been reported to be an estrogen receptor corepressor (33) and has been implicated as a tumor suppressor in breast cancer (34).

Because silencing of *SAFB* leads to decreased abundance of *FNTA* mRNA, the mechanism through which SAFB regulates *FNTA* expression appears to be at the level of transcription. However, since SAFB has been shown to bind mRNA (35, 36), stabilization of the *FNTA* message cannot be ruled out. Three independent studies have used genomic technologies to study binding sites of SAFB in the genome and regulation of gene expression. Oesterreich and colleagues investigated the role of SAFB in gene regulation in MCF-7 breast cancer cells with both ChIP-on-chip and gene expression array analyses before and after silencing *SAFB* with siRNA (22). These investigators reported 541 SAFB binding sites in promoter regions and 680 genes differentially regulated upon silencing *SAFB*. Neither *FNTA* nor *FNTB* were among the genes regulated, and gene ontogeny analysis identified immune-related genes as those most affected. Interestingly, there was no overlap between promoters identified by ChIP-on-chip and regulated genes identified by affinity microarray. The ENCODE database includes analysis of K562 cells by both ChIP-seq and RNA-seq before and after silencing *SAFB* by CRISPR-Cas9. Surprisingly, expression levels were affected in only 20% of the genes that bound SAFB, and conversely, only 28% of genes regulated by SAFB contained binding sites for the protein (*SI Appendix*, Fig. S9*B*), consistent with the earlier results of Oesterreich. Our analysis of the ENCODE expression data by gene ontology analysis revealed that the cholesterol/polyisoprene biosynthesis pathway was the most affected by SAFB deficiency (*SI Appendix*, Fig. S9*A*). This result is consistent with our KRAS4B localization screen in that *HMGCS1* and *HMGCR* were identified in both and therefore strongly supports our finding. Interestingly, *FNTA* was not observed to be regulated by SAFB in the ENCODE RNA-seq dataset. Our compelling data at the level of both mRNA and protein that demonstrate that SAFB is required for *FNTA* expression suggest either that the RNA-seq data are fraught with false negatives or there are significant cell-type differences, perhaps because SAFB functions with other, differentially expressed factors. A third

dataset available in the Gene Expression Omnibus (23) that reports RNA-seq from AML12 cells with and without silencing of *SAFB* with shRNA did reveal *FNTA* to be repressed upon loss of SAFB (albeit by only 43%). However, comparing the three sets of gene expression analyses revealed very little overlap (*SI Appendix*, Fig. S9*C*). The poor correlation of DNA binding and gene regulation suggests that SAFB may control gene expression indirectly by modulating other transcription factors or through its function as an RNA binding protein.

Our data establish SAFB as an important regulator of the protein prenylation pathway. Because *SAFB* gene products have both DNA and RNA binding domains and functions distinct from scaffold-dependent effects on chromatin (17), it is conceivable that an isolated function could be targeted therapeutically. However, we appreciate the immense technical challenge of targeting a nuclear matrix-associated protein that modulates chromatin condensation and affects expression of hundreds of genes. As such, SAFB is not an attractive target for drug discovery. Because the primary effect of SAFB on the prenylation pathway is at the level of FNTA expression, our results suggest that a therapeutic approach aimed at reducing the expression of FNTA in tumors would sensitize them to FTIs. Because FNTA is the α subunit of both FTase and GGTase 1, decreasing expression of this protein will affect both enzymes and thereby abrogate the alternative prenylation that was the basis for the failure of FTIs in the clinic (1, 9). Consistent with this model, we show that reducing FNTA expression by silencing SAFB sensitizes KRAS- and NRAS-mutant cells to growth inhibition with FTIs. Although GGTase 1 inhibitors (GGTIs) that can be combined with FTIs have been developed, as have dual FTase/GGTase 1 inhibitors, they have proven to be toxic in vivo (37). Perhaps combining FTIs with approaches aimed at diminishing FNTA expression in tumors, e.g., with protac drugs or antisense oligonucleotides, would be better tolerated than GGTIs and render RAS-driven cancers responsive to FTIs.

Methods

A summary of materials and methods is outlined below. Detailed methods can be found in *SI Appendix*.

Pooled Genome-Wide CRISPR/Cas9 Screening. The human Brunello genome-wide CRISPR knockout pooled library (one vector system, four sgRNAs per gene) was a gift from David Root and John Doench (Addgene no. 73178) (38). For screening, 2×10^8 reporter cells were infected with the lentiviral library at low multiplicity of infection such that only ∼30% of the cells survived initial puromycin selection. Cells were cultured for 9 d postinfection in the presence of 1 μg/mL puromycin and passaged with a minimum of 5×10^7 cells reseeded each time to maintain library representation. After culture, 2×10^8 live cells were sorted into GFP-positive (top 4%) and GFP-negative (all remaining cells) on a FACSAria (BD) cytometer in the Yale Flow Cytometry Facility. Genomic DNA was isolated from each population, and the sgRNA region was amplified and barcoded by PCR (38) and sequenced on an Illumina HiSeq instrument in the Yale Center for Genome Analysis. Total read counts for each condition were normalized, and total reads for each guide RNA in each population were aggregated for each gene and plotted against each other. The screen was repeated three times.

RIGER Analysis of Screening Data. The RIGER algorithm (16) in GENE-E (https://software.broadinstitute.org/GENE-E/) was used to rank each gene based on the enrichment of sgRNAs targeting that gene in the GFP positive population. To minimize error resulting from stochastic effects, sgRNAs with fewer than 100 raw reads in the GFP-positive population were excluded, and reads for each sgRNA were normalized to the total read count in the sample. Genes were ranked using the log fold change metric and the second-best hairpin method. Genes with sgRNAs that were significantly enriched ($P < 0.05$) in the GFP-positive population in each of the three independent screens were considered hits.

ENCODE Transcriptomic and Genomic Analysis. CRISPR targeted *SAFB* and nontargeting control (ENCSR336TYW, ENCSR341TTW) RNA-seq Fastq files were downloaded from ENCODE to identify deregulated genes upon deletion of *SAFB*. Paired-end reads were mapped to the hg38 reference genome using tophat/2.0.8 (39) (–no-coverage-search–no-discordant–no-mixed). Mapped reads were filtered using samtools/1.3 to retain only those with a phred score > 30. Htseq counts (40) were used to count the reads per gene using the hg38 refseq annotation of genes. The counts were then normalized using DESeq2 (41) for sequencing depth. Differentially expressed genes were identified between *SAFB*-targeted and control K562 cells using a false discovery rate of 5% and an absolute value of the $\log_2$ fold change > 1.

To identify SAFB binding sites and their putative target genes, conservative irreproducible discovery rate (IDR) peaks from SAFB ChIP-seq experiments were downloaded (ENCSR072VUO) to establish a set of reproducible SAFB binding sites across replicates. ChIPseeker (42) was used to link SAFB binding sites to genes by using a 3 kilobases window on either side of a gene's transcriptional start site. Alternatively, to annotate SAFB binding sites in intergenic regions, the Genomic Regions Enrichment of Annotations Tool (GREAT) (43) algorithm was used to link all SAFB sites to potential genes they may regulate. Finally, ChIP-seq for SAFB, H3K27ac, H3K4me1, and H3K4me3, as well as DNase-seq BigWig and bed files, were downloaded from ENCODE for visualization using the integrative genomics viewer browser (or accession IDs; see Dataset S5).

Data Availability. All study data are included in the article and *SI Appendix*.

ACKNOWLEDGMENTS. This work was funded by NIH (Grants R01CA163489, R01CA116034, and 1R35CA253178 to M.R.P.), the Yale Specialized Program of Research Excellence (SPORE) in Lung Cancer (NIH Grant P50 CA196530), the Neuwirth Beatrice Kleinberg Research Gift, and Gilead Sciences Inc.

1. A. D. Cox, C. J. Der, M. R. Philips, Targeting RAS membrane association: Back to the future for anti-RAS drug discovery? *Clin. Cancer Res.* **21**, 1819–1827 (2015).
2. B. M. Willumsen, A. Christensen, N. L. Hubbert, A. G. Papageorge, D. R. Lowy, The p21 ras C-terminus is required for transformation and membrane association. *Nature* **310**, 583–586 (1984).
3. J. H. Jackson *et al.*, Farnesol modification of Kirsten-ras exon 4B protein is essential for transformation. *Proc. Natl. Acad. Sci. U.S.A.* **87**, 3042–3046 (1990).
4. L. P. Wright, M. R. Philips, Thematic review series: Lipid posttranslational modifications. CAAX modification and membrane targeting of Ras. *J. Lipid Res.* **47**, 883–891 (2006).
5. I. M. Ahearn, K. Haigis, D. Bar-Sagi, M. R. Philips, Regulating the regulator: Post-translational modification of RAS. *Nat. Rev. Mol. Cell Biol.* **13**, 39–51 (2011).
6. I. Ahearn, M. Zhou, M. R. Philips, Posttranslational modifications of RAS proteins. *Cold Spring Harb. Perspect. Med.* **8**, a031484 (2018).
7. N. Berndt, A. D. Hamilton, S. M. Sebti, Targeting protein prenylation for cancer therapy. *Nat. Rev. Cancer* **11**, 775–791 (2011).
8. C. A. Rowell, J. J. Kowalczyk, M. D. Lewis, A. M. Garcia, Direct demonstration of geranylgeranylation and farnesylation of Ki-Ras in vivo. *J. Biol. Chem.* **272**, 14093–14097 (1997).
9. D. B. Whyte *et al.*, K- and N-Ras are geranylgeranylated in cells treated with farnesyl protein transferase inhibitors. *J. Biol. Chem.* **272**, 14459–14464 (1997).
10. I. M. Ahearn *et al.*, FKBP12 binds to acylated H-ras and promotes depalmitoylation. *Mol. Cell* **41**, 173–185 (2011).
11. A. Chandra *et al.*, The GDI-like solubilizing factor PDEδ sustains the spatial organization and signalling of Ras family proteins. *Nat. Cell Biol.* **14**, 148–158 (2011).
12. F. D. Tsai *et al.*, K-Ras4A splice variant is widely expressed in cancer and uses a hybrid membrane-targeting motif. *Proc. Natl. Acad. Sci. U.S.A.* **112**, 779–784 (2015).
13. M. Zhou *et al.*, VPS35 binds farnesylated N-Ras in the cytosol to regulate N-Ras trafficking. *J. Cell Biol.* **214**, 445–458 (2016).
14. N. Fehrenbacher *et al.*, The G protein-coupled receptor GPR31 promotes membrane association of KRAS. *J. Cell Biol.* **216**, 2329–2338 (2017).
15. T. G. Bivona *et al.*, PKC regulates a farnesyl-electrostatic switch on K-Ras that promotes its association with Bcl-XL on mitochondria and induces apoptosis. *Mol. Cell* **21**, 481–493 (2006).
16. B. Luo *et al.*, Highly parallel identification of essential genes in cancer cells. *Proc. Natl. Acad. Sci. U.S.A.* **105**, 20380–20385 (2008).
17. M. Norman, C. Rivers, Y. B. Lee, J. Idris, J. Uney, The increasing diversity of functions attributed to the SAFB family of RNA-/DNA-binding proteins. *Biochem. J.* **473**, 4271–4288 (2016).
18. B. Onken, H. Wiener, M. R. Philips, E. C. Chang, Compartmentalized signaling of Ras in fission yeast. *Proc. Natl. Acad. Sci. U.S.A.* **103**, 9045–9050 (2006).
19. M. Zhou, M. R. Philips, Nitrogen cavitation and differential centrifugation allows for monitoring the distribution of peripheral membrane proteins in cultured cells. *JoVE* 56037 (2017).
20. O. M. Khan *et al.*, Geranylgeranyltransferase type I (GGTase-I) deficiency hyperactivates macrophages and induces erosive arthritis in mice. *J. Clin. Invest.* **121**, 628–639 (2011).
21. S. Kuchay *et al.*, GGTase3 is a newly identified geranylgeranyltransferase targeting a ubiquitin ligase. *Nat. Struct. Mol. Biol.* **26**, 628–636 (2019).

22. S. Hammerich-Hille *et al*., SAFB1 mediates repression of immune regulators and apoptotic genes in breast cancer cells. *J. Biol. Chem.* **285**, 3608–3616 (2010).
23. T. Barrett *et al*., NCBI GEO: Archive for functional genomics data sets—Update. *Nucleic Acids Res.* **41**, D991–D995 (2013).
24. B. M. Willumsen, A. D. Cox, P. A. Solski, C. J. Der, J. E. Buss, Novel determinants of H-Ras plasma membrane localization and transformation. *Oncogene* **13**, 1901–1909 (1996).
25. T. K. Hayes *et al*., Long-term ERK inhibition in KRAS-mutant pancreatic cancer is associated with MYC degradation and senescence-like growth suppression. *Cancer Cell* **29**, 75–89 (2016).
26. Y. Zhou *et al*., Lipid-sorting specificity encoded in K-Ras membrane anchor regulates signal output. *Cell* **168**, 239–251.e16 (2017).
27. W. E. Kattan *et al*., Targeting plasma membrane phosphatidylserine content to inhibit oncogenic KRAS function. *Life Sci. Alliance* **2**, e201900431 (2019).
28. J. Moser von Filseck *et al*., Phosphatidylserine transport by ORP/Osh proteins is driven by phosphatidylinositol 4-phosphate. *Science* **349**, 432–436 (2015).
29. K. J. Cho *et al*., AMPK and endothelial nitric oxide synthase signaling regulates K-Ras plasma membrane interactions via cyclic GMP-dependent protein kinase 2. *Mol. Cell Biol.* **36**, 3086–3099 (2016).
30. A. Renz, F. O. Fackelmayer, Purification and molecular cloning of the scaffold attachment factor B (SAF-B), a novel human nuclear protein that specifically binds to S/MAR-DNA. *Nucleic Acids Res.* **24**, 843–849 (1996).
31. X. Huo *et al*., The nuclear matrix protein SAFB cooperates with major satellite RNAs to stabilize heterochromatin architecture partially through phase separation. *Mol. Cell* **77**, 368–383.e7 (2020).
32. A. M. Leidal *et al*., The LC3-conjugation machinery specifies the loading of RNA-binding proteins into extracellular vesicles. *Nat. Cell Biol.* **22**, 187–199 (2020).
33. S. Oesterreich *et al*., Tamoxifen-bound estrogen receptor (ER) strongly interacts with the nuclear matrix protein HET/SAF-B, a novel inhibitor of ER-mediated transactivation. *Mol. Endocrinol.* **14**, 369–381 (2000).
34. S. Oesterreich *et al*., High rates of loss of heterozygosity on chromosome 19p13 in human breast cancer. *Br. J. Cancer* **84**, 493–498 (2001).
35. A. G. Baltz *et al*., The mRNA-bound proteome and its global occupancy profile on protein-coding transcripts. *Mol. Cell* **46**, 674–690 (2012).
36. C. Rivers *et al*., iCLIP identifies novel roles for SAFB1 in regulating RNA processing and neuronal function. *BMC Biol.* **13**, 111 (2015).
37. R. B. Lobell *et al*., Evaluation of farnesyl:protein transferase and geranylgeranyl: protein transferase inhibitor combinations in preclinical models. *Cancer Res.* **61**, 8758–8768 (2001).
38. J. G. Doench *et al*., Optimized sgRNA design to maximize activity and minimize off-target effects of CRISPR-Cas9. *Nat. Biotechnol.* **34**, 184–191 (2016).
39. D. Kim *et al*., TopHat2: Accurate alignment of transcriptomes in the presence of insertions, deletions and gene fusions. *Genome Biol.* **14**, R36 (2013).
40. S. Anders, P. T. Pyl, W. Huber, HTSeq–A python framework to work with high-throughput sequencing data. *Bioinformatics* **31**, 166–169 (2015).
41. M. I. Love, W. Huber, S. Anders, Moderated estimation of fold change and dispersion for RNA-seq data with DESeq2. *Genome Biol.* **15**, 550 (2014).
42. E. G. Giannopoulou, O. Elemento, An integrated ChIP-seq analysis platform with customizable workflows. *BMC Bioinf.* **12**, 277 (2011).
43. C. Y. McLean *et al*., GREAT improves functional interpretation of cis-regulatory regions. *Nat. Biotechnol.* **28**, 495–501 (2010).